

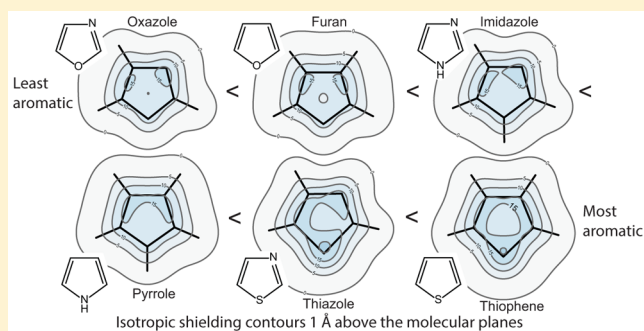
Shielding in and around Oxazole, Imidazole, and Thiazole: How Does the Second Heteroatom Affect Aromaticity and Bonding?

Kate E. Horner and Peter B. Karadakov*

Department of Chemistry, University of York, Heslington, York YO10 5DD, U.K.

S Supporting Information

ABSTRACT: Isotropic magnetic shielding distributions in the regions of space surrounding oxazole, imidazole, and thiazole are used to investigate aromaticity and bonding in these five-membered heterocycles with two heteroatoms. This is achieved by constructing HF-GIAO and MP2-GIAO (Hartree–Fock and second-order Møller–Plesset perturbation theory with gauge-including atomic orbitals) isotropic shielding plots, within the 6-311++G(d,p) basis, using regular two-dimensional 0.05 Å grids in the molecular plane and in planes 0.5 and 1 Å above it. The extent of isotropic shielding delocalization in the contour plots in planes 1 Å above the molecular plane, which is a new sensitive two-dimensional aromaticity criterion, indicates that aromaticity decreases in the order thiazole > imidazole > oxazole; in combination with previous results on furan, pyrrole, and thiophene (*J. Org. Chem.* 2013, 78, 8037–9043), the aromaticity ordering in the six five-membered heterocycles becomes thiophene > thiazole > pyrrole > imidazole > furan > oxazole. The results suggest that the inclusion of a second heteroatom in a five-membered heterocycle has a detrimental effect on its aromaticity, which is very minor in oxazole, when compared to furan, and small but noticeable in imidazole and pyrrole and in thiazole and thiophene.



INTRODUCTION

The number of known heteroaromatic compounds is surprisingly large: According to Balaban et al.,¹ about one-half of the approximately 20 million chemical compounds identified by the end of the second millennium are heteroaromatic. Despite the fact that the concepts of heteroaromaticity and aromaticity in general are very useful and frequently referred to in the chemical literature, aromaticity has proven to be notoriously difficult to define and quantify (see, for example, refs 1–5), and the search for reliable universal aromaticity criteria is unlikely to finish any time soon.

Several aromaticity criteria suggested so far are associated with the magnetic properties of aromatic systems. A well-known example is provided by the use of ¹H NMR chemical shifts to distinguish between aromatic and nonaromatic protons. NMR chemical shifts reflect the different shieldings of chemically inequivalent nuclei placed in an external magnetic field **B**₀; the magnetic field **B**_{*J*} at nucleus *J* is given by the expression

$$\mathbf{B}_J = (\mathbf{1} - \sigma_J)\mathbf{B}_0 \quad (1)$$

where σ_J is the shielding tensor of nucleus *J* (a 3 × 3 matrix with rows and columns labeled by the *x*, *y*, and *z* coordinates). Isotropic shieldings, differences between which correspond to chemical shifts, are given by one-third of the sum of the diagonal elements of the shielding tensor

$$\sigma_{J,\text{iso}} = \frac{1}{3}(\sigma_{J,xx} + \sigma_{J,yy} + \sigma_{J,zz}) \quad (2)$$

If the shielding tensor is calculated at a suitably chosen off-nucleus position **r**, the elements of the resulting $\sigma(\mathbf{r})$ can be used to define additional aromaticity criteria.

The interest in off-nucleus shielding effects dates back to the 1958 paper by Johnson and Bovey,⁶ in which they evaluated the magnetic field around benzene using Pauling's free electron model. However, calculation of shieldings at positions other than nuclei became popular much later, with the introduction of the nucleus-independent chemical shift (NICS) indices by Schleyer and co-workers.⁷ The initial NICS index, NICS(0), was defined as the isotropic shielding at a ring center with an inverted sign, $-\sigma_{\text{iso}}(\mathbf{r} = \text{ring center})$. Attempts to improve the accuracy of relative aromaticity predictions led to the formulation of further NICS indices,^{8,9} some of which have become useful aromaticity criteria. One of these is NICS(1), which is calculated similarly to NICS(0), but at a position 1 Å above the ring center, as $-\sigma_{\text{iso}}(\mathbf{r} = \text{position 1 Å above ring center})$. This repositioning eliminates most of the σ electron contributions to the index and emphasizes those of the π electrons, which are thought to be associated with aromatic ring currents. The use of NICS indices has been criticized because existing experimental techniques cannot measure shieldings at off-nucleus positions (see ref 10); it has also been suggested

Received: May 6, 2015

Published: June 17, 2015

Table 1. Isotropic Shieldings for All Nuclei in Oxazole, Imidazole, and Thiazole, Selected Nuclei in 1-Methylimidazole, and NICS(0), NICS(0.5), and NICS(1) Values (in ppm) Calculated at the HF-GIAO/6-311++G(d,p) and MP2-GIAO/6-311++G(d,p) Levels of Theory

property	oxazole (Z = O)		imidazole (Z = N)		1-methylimidazole (Z = N)		thiazole (Z = S)	
	HF	MP2	HF	MP2	HF	MP2	HF	MP2
$\sigma_{\text{iso}}(\text{Z1})$	42.7	40.1	103.7	111.1	94.8	99.8	298.1	280.8
$\sigma_{\text{iso}}(\text{C2})$	31.1	49.4	48.6	68.6	42.7	63.4	23.2	52.5
$\sigma_{\text{iso}}(\text{N3})$	-27.3	12.5	-40.1	3.7	-42.6	0.1	-106.3	-49.3
$\sigma_{\text{iso}}(\text{C4})$	60.5	71.9	57.5	69.0	53.6	65.4	44.6	56.3
$\sigma_{\text{iso}}(\text{C5})$	50.1	58.8	75.2	85.6	69.8	79.8	69.4	78.5
$\sigma_{\text{iso}}(\text{H1})$			24.2	23.5				
$\sigma_{\text{iso}}(\text{H2})$	24.3	24.4	24.5	24.6	24.6	24.8	23.1	23.6
$\sigma_{\text{iso}}(\text{H4})$	24.9	24.8	24.8	24.7	24.7	24.6	24.0	23.8
$\sigma_{\text{iso}}(\text{H5})$	24.5	24.2	25.2	25.0	25.1	24.9	25.0	24.6
NICS(0)	-11.3	-12.4	-13.8	-13.8	-13.2	-12.9	-13.0	-14.0
NICS(0.5)	-11.5	-12.4	-13.5	-13.5	-13.0	-12.8	-13.3	-14.1
NICS(1)	-9.5	-10.2	-10.9	-10.9	-10.5	-10.5	-11.2	-11.8

that describing aromaticity, which is often seen as a multidimensional property,²⁻⁵ with a single number can lead to significant information loss.¹¹ However, it is difficult to dispute the fact that NICS(1) is a reasonably accurate aromaticity index that is easy to evaluate.¹² One important feature of NICS is that the calculation does not perturb the wave function of the molecule being studied, in contrast to the discrete molecular probes used by Martin and co-workers.¹³⁻¹⁶

NICS values can be sensitive to the type of wave function used in the calculation; in particular, NICS for antiaromatic compounds cannot be evaluated correctly with the Hartree-Fock (HF) method or density functional theory (DFT) and require appropriate CASSCF or MCSCF (complete-active-space or multiconfiguration self-consistent field) wave functions.^{17,18} The quality of the basis set can also affect the results of NICS-based analyses; for example, it has been shown that use of limited basis sets can lead to a predicted ordering of the aromaticities of furan, pyrrole, and thiophene, which is inconsistent with that suggested by experimental data.¹⁹

One way to avoid the NICS problem of reducing aromaticity to a single number is to study the variation of $\sigma_{\text{iso}}(\mathbf{r})$ throughout the region of space surrounding an aromatic or antiaromatic molecule. Kleinpeter et al. used regular grids of $\sigma_{\text{iso}}(\mathbf{r})$ values with a relatively wide spacing (0.5 Å) to generate isotropic chemical shielding surfaces (ICSSs)²¹⁻²⁴ for a number of molecules; the ICSSs were then employed to analyze aromaticity and antiaromaticity, diatropic and paratropic regions within molecules, the anisotropic effects due to specific substituents, etc.

More recent research^{19,25} has demonstrated that the construction of $\sigma_{\text{iso}}(\mathbf{r})$ isosurfaces utilizing much denser regular grids of $\sigma_{\text{iso}}(\mathbf{r})$ values (spacing of 0.05 Å) makes it possible to observe subtle features of the isotropic shielding around a molecule, which cannot be seen in the ICSSs constructed using coarser grids by Kleinpeter and co-workers. The more detailed $\sigma_{\text{iso}}(\mathbf{r})$ isosurfaces and the associated $\sigma_{\text{iso}}(\mathbf{r})$ contour plots allow very clear distinction between aromatic and antiaromatic systems and comparisons between the relative degrees of aromaticity of heterocycles such as furan, pyrrole, and thiophene. The results are consistent with experimental data and furnish additional insights into chemical bonding, including the extent to which it is affected by aromaticity and antiaromaticity.²⁵

As a number of biologically important heterocycles contain multiple heteroatoms, it is not surprising that the aromaticities of three common five-membered heterocycles with two heteroatoms, oxazole, imidazole, and thiazole have been the subject of several investigations making use of different aromaticity criteria.

In contrast to the difference expected from experimental resonance energies, Bird's statistical analysis of bond orders suggested that imidazole and thiazole should exhibit similar levels of aromaticity (see ref 20 and references therein). This result illustrates the recognized fact that aromaticity cannot be described reliably using only structural parameters; another example is provided by benzene and borazine, both of which feature complete bond equalization but show very different aromaticities.

According to Jug's bond-order criterion for ring current effects,²⁶ aromaticity should decrease in the order pyrrole > thiophene > furan > imidazole > oxazole > thiazole.² The alternative bond-valence criterion suggests a modified sequence: thiophene > pyrrole > thiazole > furan > imidazole > oxazole.² The positions of thiophene, pyrrole, and furan within this modified sequence are in agreement with the experimental observations about the reactivities of these molecules. The modified sequence is also supported by the magnitudes of the out-of-plane component of the magnetic susceptibility tensor, χ_{zz} , calculated for some of its members, according to which pyrrole > furan > imidazole > oxazole.²

Analyses of the aromaticity of five-membered heterocycles using structural and energetic criteria suggest that aromaticity decreases with the increase of the difference between the electronegativities of a heteroatom and its neighboring atoms.^{27,28} Two further observations are that, in general, adding nitrogens to a heterocycle increases its aromaticity (however, furan is considered to be more aromatic than oxazole) and that the degree of aromaticity is determined mainly by the heteroatom donating two π electrons to the conjugated system.²⁸

The aim of this paper is to present a thorough analysis of the behavior of the isotropic shielding $\sigma_{\text{iso}}(\mathbf{r})$ in and around oxazole, imidazole, and thiazole and use the results to explain the differences in aromaticity and bonding in these molecules. The outcomes of this analysis are compared to those from an earlier study of aromatic five-membered heterocycles with one heteroatom.¹⁹

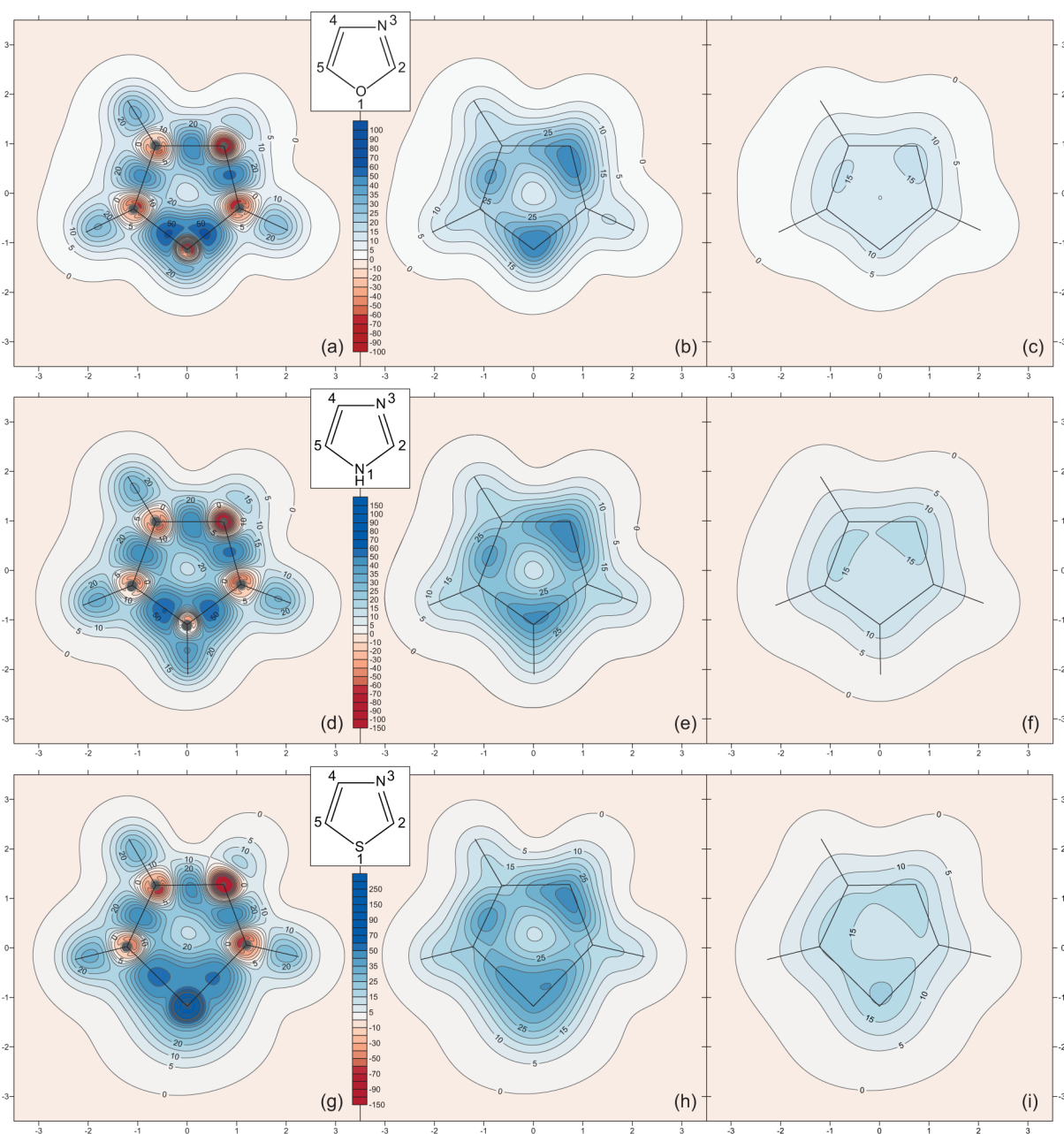


Figure 1. Contour plots of the isotropic shielding $\sigma_{\text{iso}}(\mathbf{r})$ (in ppm) for oxazole (a–c), imidazole (d–f), and thiazole (g–i) in the respective molecular planes (a,d,g) and planes 0.5 Å (b,e,h) and 1 Å (c,f,i) above the molecular planes.

■ COMPUTATIONAL PROCEDURE

The on- and off-nucleus gas-phase isotropic magnetic shielding values reported in this paper were evaluated using two methods, HF and second-order Møller–Plesset perturbation theory (MP2). In both cases, the molecular orbitals were expanded in terms of gauge-including atomic orbitals (GIAOs). All HF-GIAO and MP2-GIAO calculations were carried out within the 6-311++G(d,p) basis set by means of Gaussian 09,²⁹ under the “SCF(Tight)” convergence criterion and with the “CPHF(Separate)” keyword. For thiazole, use was made of the C_s experimental gas-phase ground-state equilibrium geometry determined through microwave spectroscopy.³⁰ The gas-phase C_s ground-state geometries of oxazole, imidazole, and 1-methylimidazole (which was used to compare our calculated carbon and nitrogen shieldings to existing experimental and theoretical data) were optimized with Gaussian 09 at the MP2(FC)/aug-cc-pVTZ level of theory (“FC” stands for frozen-core) using the “VeryTight” convergence criteria. The optimized geometries were confirmed to be

local minima through diagonalizations of the corresponding analytic nuclear Hessians.

Detailed contour plots depicting the changes in isotropic shielding in the regions of space most relevant to chemical bonding and aromaticity surrounding oxazole, imidazole, and thiazole were obtained by evaluating $\sigma_{\text{iso}}(\mathbf{r})$ at regular $7 \text{ \AA} \times 6.5 \text{ \AA}$ two-dimensional grids of points with spacing of 0.05 \AA in three planes, the molecular plane as well as two planes parallel to the molecular plane at heights of 0.5 and 1 Å above it, respectively.

The grid points are specified in the Gaussian 09 input as ghost atoms without basis functions (symbol “Bq”). As the Gaussian 09 input routines limit the number of ghost atoms within a single geometry specification, it was necessary to perform a series of separate NMR calculations including 95 ghost atoms each. The set of input files for each molecule was prepared by means of a purpose-written program.

RESULTS AND DISCUSSION

The isotropic shieldings for all nuclei in oxazole, imidazole, and thiazole and selected nuclei in 1-methylimidazole are shown in Table 1, together with the NICS(0), NICS(0.5) (NICS calculated at a height of 0.5 Å above the ring center), and NICS(1) values. Heavy atoms are numbered counterclockwise, as shown in Figure 1; ring hydrogens are labeled with the numbers of the heavy atoms to which they are attached. The NICS values were calculated at and above the geometric centers of the five-membered rings, located by averaging the coordinates of the heavy atoms forming each ring.

The N3 nucleus present in all four heterocycles is strongly deshielded; in imidazole, at the HF-GIAO and MP2-GIAO levels of theory, its isotropic shielding is lower than that of the N1 nucleus by ca. 144 and 107 ppm, respectively. According to solid-state ¹⁵N NMR experimental data, the difference between the nitrogen isotropic shieldings in imidazole is 76 ppm;³¹ one of the reasons for the gap between the experimental solid-state and gas-phase MP2-GIAO values is the presence of hydrogen bonding in crystalline imidazole, which makes the environments of the two nitrogens less dissimilar. It is difficult to compare the theoretical gas-phase nitrogen shieldings for imidazole to liquid-state NMR measurements as most of these are in aqueous solutions where, due to annular tautomerism, the N1 and N3 nuclei become magnetically equivalent.³² Comparisons of this type are easier for an imidazole derivative, 1-methylimidazole, for which there is extensive experimental and theoretical nitrogen NMR data.^{33–35} The difference between the N1 and N3 shieldings in 1-methylimidazole, measured in cyclohexane by Witanowski et al.,³³ amounts to 113.52 ppm. Surprisingly, the gas-phase HF-GIAO/6-31++G(d,p)//HF/6-31++G(d,p) estimate of this difference, 122.5 ppm,³⁴ is better than our HF-GIAO difference of 137.4 ppm obtained using a larger basis set, 6-311++G(d,p), and for a geometry optimized at a higher level of theory, MP2(FC)/aug-cc-pVTZ. A more accurate gas-phase RASSCF-GIAO/HII//MP2/6-311G(d,p) calculation (using a restricted active-space self-consistent field wave function with the Huzinaga HII basis set) places the $\sigma_{\text{iso}}(\text{N1}) - \sigma_{\text{iso}}(\text{N3})$ difference at 111.64 ppm.³⁵ Despite the fact that our HF-GIAO and MP2-GIAO calculations overestimate and underestimate the difference between the experimentally measured N1 and N3 shieldings at 137.4 and 99.7 ppm, respectively, it is possible to use these numbers in order to obtain an improved theoretical value for this difference: As the correlation corrections to isotropic shieldings obtained at the MP2-GIAO level of theory are often too large, Chesnut has suggested³⁶ an approximate infinite-order perturbation theory prescription for estimating isotropic shieldings³⁶ from HF-GIAO and MP2-GIAO results, which takes the form

$$\sigma_{\text{iso}}^{\text{MP}\infty} = \sigma_{\text{iso}}^{\text{HF}} + \frac{2}{3}(\sigma_{\text{iso}}^{\text{MP2}} - \sigma_{\text{iso}}^{\text{HF}}) \quad (3)$$

If we apply Chesnut's expression 3 to our HF-GIAO and MP2-GIAO results for 1-methylimidazole, the "MP ∞ " difference between the N1 and N3 shieldings becomes 112.3 ppm, which is in very good agreement with the experiment.

In all four heterocycles, the most deshielded carbons are those connected to two heteroatoms (C2). The C5 carbons are more shielded than the C4 carbons in imidazole, 1-methylimidazole, and thiazole; in oxazole, the bond to the strongly electronegative oxygen makes C5 less shielded than

C4. At the MP2-GIAO level of theory, the differences between $\sigma_{\text{iso}}(\text{C2})$ and $\sigma_{\text{iso}}(\text{C4})$ decrease, especially in imidazole, 1-methylimidazole, and thiazole, but the differences between $\sigma_{\text{iso}}(\text{C4})$ and $\sigma_{\text{iso}}(\text{C5})$, which are engaged in a carbon–carbon "double" bond, remain substantial, in contrast to the situation encountered in furan, pyrrole, and thiophene.¹⁹

The differences between our HF-GIAO and MP2-GIAO isotropic shieldings for the C2, C4, and C5 nuclei in oxazole, imidazole, 1-methylimidazole, and thiazole and the differences between the respective experimental liquid-state NMR chemical shifts are summarized in Table 2. The $\delta(\text{C2}) - \delta(\text{C4})$ and

Table 2. Differences between ¹³C Experimental Chemical Shifts (δ) and Theoretical Isotropic Shieldings for Oxazole, Imidazole, 1-Methylimidazole, and Thiazole (in ppm)^a

property	oxazole	imidazole	1-methylimidazole	thiazole
$\delta(\text{C2}) - \delta(\text{C4})$ (exptl ^b)	25.2	13.9	9.1	10.3
$\sigma_{\text{iso}}(\text{C4}) - \sigma_{\text{iso}}(\text{C2})$ (HF)	29.4	8.9	13.0	21.4
$\sigma_{\text{iso}}(\text{C4}) - \sigma_{\text{iso}}(\text{C2})$ (MP2)	22.5	0.4	4.1	3.8
$\sigma_{\text{iso}}(\text{C4}) - \sigma_{\text{iso}}(\text{C2})$ (MP ∞)	24.8	3.2	7.1	9.7
$\delta(\text{C2}) - \delta(\text{C5})$ (exptl ^b)	12.5	13.9	17.5	34.0
$\sigma_{\text{iso}}(\text{C5}) - \sigma_{\text{iso}}(\text{C2})$ (HF)	19.0	26.6	24.7	46.2
$\sigma_{\text{iso}}(\text{C5}) - \sigma_{\text{iso}}(\text{C2})$ (MP2)	9.4	17.0	14.2	26.0
$\sigma_{\text{iso}}(\text{C5}) - \sigma_{\text{iso}}(\text{C2})$ (MP ∞)	12.6	20.3	17.7	32.7

^aHF and MP2 stand for HF-GIAO/6-311++G(d,p) and MP2-GIAO/6-311++G(d,p), respectively; MP ∞ denotes extrapolated shieldings obtained by eq 3. ^bThe experimental ¹³C chemical shifts for oxazole and 1-methylimidazole were taken from ref 37 (measured in CDCl₃), and those for thiazole come from ref 38 (measured in DMSO-*d*₆). For imidazole, we quote the aqueous solution values from ref 39, noting that, due to annular tautomerism, $\delta(\text{C4}) = \delta(\text{C5})$.

$\delta(\text{C2}) - \delta(\text{C5})$ differences fall between the respective HF-GIAO and MP2-GIAO $\sigma_{\text{iso}}(\text{C4}) - \sigma_{\text{iso}}(\text{C2})$ and $\sigma_{\text{iso}}(\text{C5}) - \sigma_{\text{iso}}(\text{C2})$ differences for all molecules except imidazole, for which, in aqueous solutions, C2 and C4 (just as N1 and N3, vide supra) are magnetically equivalent. Once again, Chesnut's extrapolation 3 markedly improves the agreement between theory and experiment.

The good agreement between our theoretical NMR results and experimental nitrogen and carbon NMR data shows that the level of theory we have chosen ensures sufficient accuracy, especially if augmented with eq 3. The quality of the theoretical estimates for the C, N, O, and S isotropic shieldings can be improved further by using higher levels of theory, such as CCSD(T)-GIAO,⁴⁰ and/or larger basis sets, but it is likely that the improvements will be relatively modest in comparison to the "MP ∞ " values.

The proton shieldings calculated at the HF-GIAO and MP2-GIAO levels of theory are very close, within 0.5 ppm of one another; a similar trend is followed by the NICS(0), NICS(0.5), and NICS(1) values, which vary by no more than 1.1 ppm between the two levels of theory (see Table 1). In general, while the differences between HF-GIAO and MP2-GIAO isotropic shieldings for heavy nuclei can be large, proton and off-nucleus shieldings calculated at these two levels of theory are very similar, especially in regions away from heavy nuclei. Due to this similarity, we present and discuss only $\sigma_{\text{iso}}(\mathbf{r})$ contour plots obtained at the higher level of theory.

Clearly, the application of Chesnut's expression 3 would change the MP2-GIAO proton and off-nucleus shieldings very little, and there is no need to do this. As the shielding calculations on 1-methylimidazole were carried out in order to facilitate the comparison between experimental and theoretical NMR results, we are not going to discuss this imidazole derivative any further.

According to Nyulászai et al.,²⁸ for systems with more than one heteroatom, such as oxazole, imidazole, and thiazole, the "first" heteroatom (Z1), which donates two π electrons to the conjugated system, has a more pronounced contribution to ring aromaticity than the "second" heteroatom (N3). However, the substantial deshielding of the nucleus of the "second" heteroatom (N3) in all three heterocycles indicates that its surroundings interact strongly with the rest of the molecule. This suggests that previous work may have underestimated the influence of the "second" heteroatom on ring aromaticity.

The HF-GIAO NICS(0) and NICS(0.5) values suggest that aromaticity decreases in the order imidazole > thiazole > oxazole (see Table 1). However, according to the MP2-GIAO NICS(0), NICS(0.5), NICS(1), and HF-GIAO NICS(1) values, thiazole is more aromatic than imidazole, and the ordering changes to thiazole > imidazole > oxazole. It is obvious that the NICS(1) index differentiates best between the relative aromaticities of the three heterocycles, which highlights the importance of eliminating, as far as possible, σ electron contributions to the isotropic shielding when using it to describe aromaticity. It can also be argued that the MP2-GIAO NICS values, which include dynamic correlation effects, are more reliable than those calculated at the HF-GIAO level, as the aromaticity ordering is consistent throughout the MP2-GIAO-level NICS(0), NICS(0.5), and NICS(1) ranges. The different predictions about the relative aromaticities of imidazole and thiazole obtained by means of different NICS indices reiterate how difficult it is to reduce a global property such as aromaticity to a single numerical value, as previously discussed.^{19,25}

Combining the MP2-GIAO/6-311++G(d,p) NICS(1) values for oxazole, imidazole, and thiazole from the current work with the NICS(1) values for furan, pyrrole, and thiophene from ref 19, obtained at the same level of theory, yields the following ordering of relative aromaticities: thiazole (−11.8) > thiophene (−11.7) > imidazole (−10.9) > pyrrole (−10.2) \approx oxazole (−10.2) > furan (−9.7) [NICS(1) values in ppm in brackets]. While, according to NICS(1), each of the heterocycles containing two heteroatoms is predicted to be more aromatic than its counterpart involving a single heteroatom, the differences between the respective NICS(1) values are very small, between 0.1 and 0.7 ppm.

More detailed information about the aromaticities of oxazole, imidazole, and thiazole and chemical bonding in these molecules can be obtained by analyzing the contour plots of the isotropic shielding $\sigma_{\text{iso}}(\mathbf{r})$ in the molecular plane and the planes 0.5 and 1 Å above the molecular plane for each molecule, shown in Figure 1.

The $\sigma_{\text{iso}}(\mathbf{r})$ contour plots in the molecular plane for all three azoles show increased shielding along the σ bond framework. The most shielded regions surround the bonds between the "first" heteroatom (Z1) and its neighbors, C2 and C5, followed by the regions encompassing the C2–N3 bonds. This observation is supported by the highest $\sigma_{\text{iso}}(\mathbf{r})$ values within carbon–heteroatom and carbon–carbon bonding regions shown in Table 3. Although the isotropic shielding variations

Table 3. Highest Isotropic Shieldings within Carbon–Heteroatom and Carbon–Carbon Bonding Regions in Oxazole, Imidazole, and Thiazole (in ppm)^a

bond	highest $\sigma_{\text{iso}}(\mathbf{r})$ value		
	oxazole (Z = O)	imidazole (Z = NH)	thiazole (Z = S)
Z1–C2	64	59	52
C2–N3	53	53	48
N3–C4	46	49	43
C4–C5	44	47	47
C5–Z1	62	61	54

^aApproximate values taken from the $\sigma_{\text{iso}}(\mathbf{r})$ grids in the respective molecular planes calculated at the MP2-GIAO/6-311++G(d,p) level of theory.

in the molecular plane suggest that Z1–C2 and C5–Z1 are the strongest σ bonds in oxazole, imidazole, and thiazole, the shortest bond length in each of these heterocycles corresponds to the C2–N3 bond. A partial explanation follows from an examination of the $\sigma_{\text{iso}}(\mathbf{r})$ contour plots above the molecular plane: The increased out-of-plane shielding over the C2–N3 and C4–C5 bonds can be associated with stronger π bonding interactions. However, while this simple qualitative analysis shows that there are good grounds for identifying all C2–N3 bonds and the C4–C5 bonds in oxazole and thiazole as formally "double", it does not help us understand why the C4–C5 bond in imidazole is the longest bond in the ring. Another interesting feature of the $\sigma_{\text{iso}}(\mathbf{r})$ contour plots in the molecular plane is the rather uniform isotropic shielding distribution along the bonds within the C5–Z1–C2–N3 and N3–C4–C5 fragments in oxazole and imidazole and within the C5–S1–C2 and C2–N1–C4–C5 fragments in thiazole (see also Table 3). The degrees of uniformity are similar to those along the bonds in the oxazole, imidazole, and thiophene rings,¹⁹ slightly lower than that in the benzene ring,^{19,25} and suggest stable σ bond frameworks.

The isotropic shielding contour plots in the molecular planes of oxazole, imidazole, and thiazole show the deshielded "halos" around sp^2 -hybridized second-row atoms that have been described previously.^{19,25} Similarly to thiophene,¹⁹ there is no such "halo" around the sulfur nucleus in thiazole. In line with the data presented in Table 1, the most deshielded region in each of the three heterocycles surrounds the N nucleus. This is another illustration of the extent to which the presence of the "second" heteroatom influences the electronic structures of oxazole, imidazole, and thiazole. In relative terms, the regions around the N nuclei in oxazole, imidazole, and, especially, thiazole exhibit the most pronounced deshielded "halos" around sp^2 -hybridized second-row atoms that have been observed so far.

All three $\sigma_{\text{iso}}(\mathbf{r})$ contour plots in the molecular plane (Figure 1a,d,g) hint at the presence of in-plane lone pairs at the N atoms. However, the regions of space that can be associated with these lone pairs are much less shielded than those along C–H and N–H bonds. Still, the N lone pairs are easier to distinguish than the in-plane lone pairs on O in oxazole and S in thiazole.

Traditionally, aromaticity has been regarded as a property associated mainly with the π electrons. Clearly, the shapes of the $\sigma_{\text{iso}}(\mathbf{r})$ contour plots in the molecular planes of oxazole, imidazole, and thiazole are determined predominantly by σ electron contributions. More information about the π electron contributions to the isotropic shielding distributions around

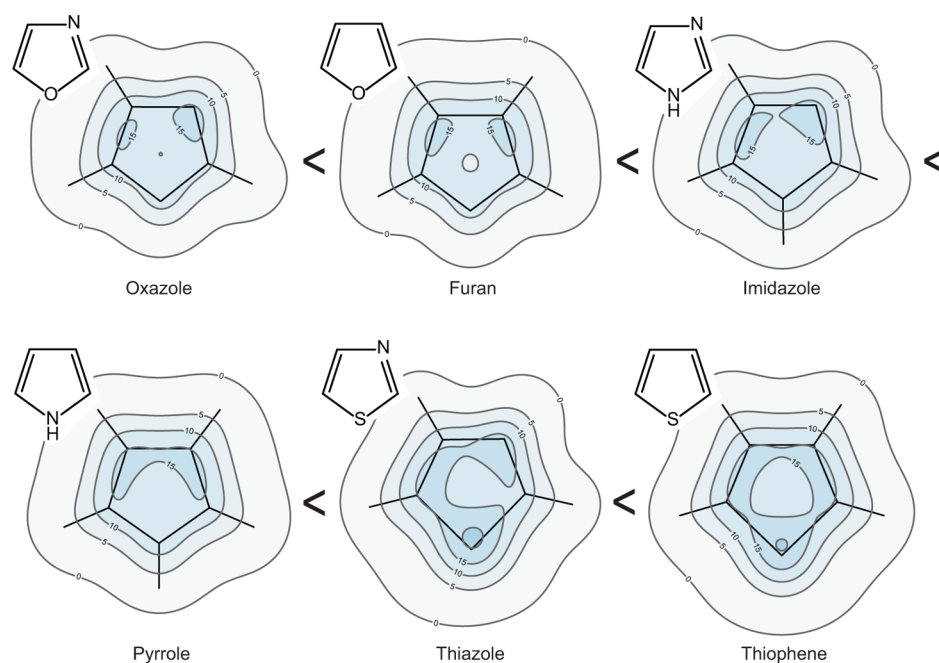


Figure 2. Relative aromaticities of furan, pyrrole, thiophene, oxazole, imidazole, and thiazole suggested by the extent of $\sigma_{\text{iso}}(\mathbf{r})$ delocalization in the isotropic shielding contour plots in planes 1 Å above the molecular plane.

these azoles can be obtained by studying the $\sigma_{\text{iso}}(\mathbf{r})$ contour plots in planes 0.5 and 1 Å above the molecular plane. The $\sigma_{\text{iso}}(\mathbf{r})$ shielding map at a height of 0.5 Å above the molecular plane is influenced by both σ and π electrons: Contour plots in Figure 1b,e,h highlight the positions of the π bonds and π lone pairs and do not show any deshielded “halos” around C, N, and O atoms; however, it is still easy to distinguish the outlines of all C–H and N–H bonds. There are next to no visible σ electron contributions in the isotropic shielding contour plots in planes 1 Å above the molecular planes of oxazole, imidazole, and thiazole (Figure 1c,f,i). The heavy atom frameworks in all three molecules are under areas of increased isotropic shielding (over 10 ppm), which include regions of even higher $\sigma_{\text{iso}}(\mathbf{r})$ values (over 15 ppm). There are two relatively small $\sigma_{\text{iso}}(\mathbf{r}) \geq 15$ ppm regions in oxazole, two bulkier and almost connected regions of this type in imidazole, and a much larger single $\sigma_{\text{iso}}(\mathbf{r}) \geq 15$ ppm region in thiazole, which encompasses most of the area above the ring. Thus, the increased isotropic shielding at a height of 1 Å above the molecular plane is most uniformly delocalized in thiazole, followed by imidazole and oxazole. As a consequence of the link between aromaticity and isotropic shielding delocalization, established in ref 19, these results indicate that the three azoles are ordered, in terms of relative aromaticity, as thiazole > imidazole > oxazole. Our finding that thiazole is significantly more aromatic than imidazole and oxazole is in agreement with experimental evidence indicating that thiazole is much less reactive than imidazole, which, in turn, is often less reactive than oxazole (for example, oxazoles readily undergo Diels–Alder-type cycloaddition reactions across the 2,5-positions, which are not observed for thiazole and imidazole).⁴¹ These reactivity trends have also been confirmed by the results of a recent theoretical study of the reactivity patterns of imidazole, oxazole, and thiazole through polarization justified Fukui functions.⁴²

At this moment, it is appropriate to compare the isotropic shielding maps in planes 1 Å above the molecular planes for oxazole, imidazole, and thiazole to the respective maps for

furan, pyrrole, and thiophene.¹⁹ MP2-GIAO/6-311++G(d,p) data from the current work and ref 19 were used to prepare the contour plots presented in Figure 2. The extents of isotropic shielding delocalization observed in the contour plots for oxazole and furan are very similar and noticeably lower than those in the other four heterocycles. A closer look at oxazole shows that the presence of the second heteroatom (N3) distorts the $\sigma_{\text{iso}}(\mathbf{r})$ contours corresponding to 0, 5, and 10 ppm and shifts one of the $\sigma_{\text{iso}}(\mathbf{r}) = 15$ ppm contours toward the region above the N nucleus. The area enclosed by the $\sigma_{\text{iso}}(\mathbf{r}) = 15$ ppm contour over the C4–C5 bond is noticeably smaller than the corresponding area in oxazole. The area enclosed by the $\sigma_{\text{iso}}(\mathbf{r}) = 15$ ppm contour over the C2–N3 bond is of very much the same size as its counterpart in oxazole, but its shape and position suggest that it is partially localized over the N3 nucleus. As a result of these observations, furan can be classified as slightly more aromatic than oxazole. The differences between the contour plots for imidazole and pyrrole are more pronounced and suggest that pyrrole is more aromatic than imidazole; similarly, thiophene is predicted to be more aromatic than thiazole. Thus, in terms of relative aromaticity, the six heterocycles are ordered as thiophene > thiazole > pyrrole > imidazole > furan > oxazole. This ordering suggests that the inclusion of a second heteroatom in a five-membered heterocycle has a detrimental effect on its aromaticity, which can be very minor as in the case of oxazole, when compared to furan, or small but noticeable as in imidazole and pyrrole, and thiazole and thiophene. In this aspect, the ordering of relative aromaticities following from the extents of isotropic shielding delocalization in planes 1 Å above the molecular planes differs from the NICS(1) classification (vide supra), according to which the inclusion of a second heteroatom leads to a slight increase in the aromaticity of a five-membered heterocycle. Having in mind the fact that the use of any NICS index, including NICS(1), is equivalent to reducing aromaticity, which is a global property, to a single numerical value, our two-dimensional approach, which identifies areas associated with

more intense presence and movement of π electrons in a plane 1 Å above the molecular plane, can be expected to yield more accurate and consistent results.

CONCLUSIONS

The analysis of the isotropic shielding $\sigma_{\text{iso}}(\mathbf{r})$ variations within the regions of space surrounding oxazole, imidazole, and thiazole, three common five-membered heterocycles with two heteroatoms, provides useful insights into the way in which the presence of the second heteroatom (nitrogen) affects chemical bonding and aromaticity. The second heteroatoms in imidazole, oxazole, and thiazole are strongly deshielded, and so are their surroundings; in comparison to the five-membered heterocycles with one heteroatom, furan, pyrrole, and thiophene,¹⁹ the introduction of the second heteroatom leads to a significant perturbation of the isotropic shielding distribution in and around the molecule.

The $\sigma_{\text{iso}}(\mathbf{r})$ contour plots in the molecular planes of oxazole, imidazole, and thiazole show regions of increased shielding along all bonds, which suggest stable σ bond frameworks. It was interesting to observe that, while these contour plots hint at the presence of in-plane lone pairs at the nitrogen atoms, the regions of space that can be associated with these lone pairs are much less shielded than those along C–H and N–H bonds.

The comparison between the $\sigma_{\text{iso}}(\mathbf{r})$ contour plots in planes 1 Å above the molecular planes in oxazole, imidazole, and thiazole obtained in the current work and previous results for furan, pyrrole, and thiophene¹⁹ shows that, according to the extent of isotropic shielding delocalization observed in these plots, aromaticity decreases in the order thiophene > thiazole > pyrrole > imidazole > furan > oxazole. While it is logical to expect that the introduction of a second heteroatom in furan, pyrrole, and thiophene, yielding oxazole, imidazole, and thiazole, respectively, would have, in each case, a detrimental effect on aromaticity, as it impedes the ability of the π electrons to delocalize, it is surprising to observe that a number of aromaticity criteria that measure aromaticity through a single number, including NICS(1), make the opposite prediction. This is due to the fact that, as our analysis indicates, the differences between the relative aromaticities of the pairs furan and oxazole, pyrrole and imidazole, and thiophene and thiazole are small and could be misinterpreted by approaches that measure aromaticity through a single numerical value.

Arguably, the two-dimensional nature of our approach, which is based on comparisons between the extent of isotropic shielding delocalization in planes 1 Å above the molecular planes and can be thought of, on the basis of the results reported in the current work and in ref 19, as a promising new aromaticity criterion, allows it to differentiate between systems with similar aromaticities in a more accurate and consistent way than most of the existing aromaticity criteria.

ASSOCIATED CONTENT

Supporting Information

Gaussian 09 route section used in all MP2-GIAO calculations. Cartesian coordinates, HF and MP2 total energies, and HF-GIAO MP2-GIAO shielding tensors for oxazole, imidazole, 1-methylimidazole, and thiazole, including NICS(0), NICS(0.5), and NICS(1) values, taken from the Gaussian 09 MP2-GIAO output files. The Supporting Information is available free of charge on the ACS Publications website at DOI: 10.1021/acs.joc.5b01010.

AUTHOR INFORMATION

Corresponding Author

*Phone: +44 1904 322555. E-mail: peter.karakakov@york.ac.uk.

Notes

The authors declare no competing financial interest.

ACKNOWLEDGMENTS

The authors thank the Department of Chemistry of the University of York for a Teaching Scholarship to K.E.H.

REFERENCES

- (1) Balaban, A. T.; Oniciu, D. C.; Katritzky, A. R. *Chem. Rev.* **2004**, *104*, 2777–2812.
- (2) Jug, K.; Koster, A. M. *J. Phys. Org. Chem.* **1991**, *4*, 163–169.
- (3) Katritzky, A. R.; Karelson, M.; Sild, S.; Krygowski, T. M.; Jug, K. *J. Org. Chem.* **1998**, *63*, 5228–5231.
- (4) Cyrański, M. K.; Krygowski, T. M.; Katritzky, A. R.; Schleyer, P. v. R. *J. Org. Chem.* **2002**, *67*, 1333–1338.
- (5) Chen, Z.; Wannere, C. S.; Corminboeuf, C.; Puchta, R.; Schleyer, P. v. R. *Chem. Rev.* **2005**, *105*, 3842–3888.
- (6) Johnson, C. E.; Bovey, F. A. *J. Chem. Phys.* **1958**, *29*, 1012–1014.
- (7) Schleyer, P. v. R.; Maerker, C.; Dransfeld, A.; Jiao, H.; Hommes, N. J. R. v. E. *J. Am. Chem. Soc.* **1996**, *118*, 6317–6318.
- (8) Schleyer, P. v. R.; Jiao, H.; Hommes, N. J. R. v. E.; Malkin, V. G.; Malkina, O. L. *J. Am. Chem. Soc.* **1997**, *119*, 12669–12670.
- (9) Schleyer, P. v. R.; Manoharan, M.; Wang, Z. X.; Kiran, B.; Jiao, H.; Puchta, R.; Hommes, N. J. R. v. E. *Org. Lett.* **2001**, *3*, 2465–2468.
- (10) Lazzarotti, P. *Phys. Chem. Chem. Phys.* **2004**, *6*, 217–223.
- (11) Fias, S.; Fowler, P. W.; Delgado, J. L.; Hahn, U.; Bultinck, P. *Chem.—Eur. J.* **2008**, *14*, 3093–3099.
- (12) Fallah-Bagher-Shaidaei, H.; Wannere, C. S.; Corminboeuf, C.; Puchta, R.; Schleyer, P. v. R. *Org. Lett.* **2006**, *8*, 863.
- (13) Martin, N. H.; Brown, J. D.; Nance, K. H.; Schaefer, H. F.; Schleyer, P. v. R.; Wang, Z. X.; Woodcock, H. L. *Org. Lett.* **2001**, *3*, 3823–3826.
- (14) Martin, N. H.; Loveless, D. M.; Main, K. L.; Wade, D. C. *J. Mol. Graphics Modell.* **2006**, *25*, 389–395.
- (15) Martin, N. H.; Rowe, J. E.; Pittman, E. L. *J. Mol. Graphics Modell.* **2009**, *27*, 853–859.
- (16) Martin, N. H.; Teague, M. R.; Mills, K. H. *Symmetry* **2010**, *2*, 418–436.
- (17) Karadakov, P. B. *J. Phys. Chem. A* **2008**, *112*, 7303–7309.
- (18) Karadakov, P. B. *J. Phys. Chem. A* **2008**, *112*, 12707–12713.
- (19) Horner, K. E.; Karadakov, P. B. *J. Org. Chem.* **2013**, *78*, 8037–8043.
- (20) Bird, C. W. *Tetrahedron* **1985**, *41*, 1409–1414.
- (21) Klod, S.; Kleinpeter, E. *J. Chem. Soc., Perkin Trans. 2* **1989**, 1893–1898.
- (22) Kleinpeter, E.; Klod, S.; Koch, A. *J. Mol. Struct. THEOCHEM* **2007**, *811*, 45–60.
- (23) Kleinpeter, E.; Koch, A. *Phys. Chem. Chem. Phys.* **2012**, *14*, 8742–8746.
- (24) Kleinpeter, E.; Koch, A. *J. Phys. Chem. A* **2012**, *116*, 5674–5680.
- (25) Karadakov, P. B.; Horner, K. E. *J. Phys. Chem. A* **2013**, *117*, 518–523.
- (26) Jug, K. *J. Org. Chem.* **1983**, *48*, 1344–1348.
- (27) Simkin, B. Y.; Minkin, V. I.; Glukhovtsev, M. N. In *Advances in Heterocyclic Chemistry*; Katritzky, A. R., Ed.; Academic Press: San Diego, CA, 1993; Vol. 56, pp 303–428.
- (28) Nyulászi, L.; Varnai, P.; Veszpremi, T. *J. Mol. Struct. THEOCHEM* **1995**, *358*, 55–61.
- (29) Frisch, M. J.; Trucks, G. W.; Schlegel, H. B.; Scuseria, G. E.; Robb, M. A.; Cheeseman, J. R.; Scalmani, G.; Barone, V.; Mennucci, B.; Petersson, G. A.; et al. *Gaussian 09*, revision B.01; Gaussian, Inc.: Wallingford, CT, 2009.

- (30) Nygaard, L.; Asmussen, E.; Høg, J. H.; Maheshwari, R. C.; Nielsen, C. H.; Petersen, I. B.; Rastrup-Andersen, J.; Sørensen, G. O. *J. Mol. Struct.* **1971**, *8*, 225–233.
- (31) Hickman, B. S.; Mascal, M.; Titman, J. J.; Wood, I. G. *J. Am. Chem. Soc.* **1999**, *121*, 11486–11490.
- (32) Alei, M., Jr.; Morgan, L. O.; Wageman, W. E. *Inorg. Chem.* **1978**, *17*, 2288–2293.
- (33) Witanowski, M.; Sicinska, W.; Biedrzycka, Z.; Webb, G. A. *J. Magn. Reson. A* **1994**, *109*, 177–180.
- (34) Witanowski, M.; Biedrzycka, Z.; Sicinska, W.; Grabowski, Z. *J. Magn. Reson.* **1998**, *131*, 54–60.
- (35) Jaszuński, M.; Mikkelsen, K. V.; Rizzo, A.; Witanowski, M. *J. Phys. Chem. A* **2000**, *104*, 1466–1473.
- (36) Chesnut, D. B. *Chem. Phys. Lett.* **1995**, *246*, 235–238.
- (37) Hiemstra, H.; Houwing, H. A.; Possel, O.; van Leusen, A. M. *Can. J. Chem.* **1979**, *57*, 3168–3170.
- (38) Faure, R.; Galy, J.-P.; Vincent, J.; Elguero, J. *Can. J. Chem.* **1978**, *56*, 46–55.
- (39) Wasylishen, R. E.; Graham, M. R. *Can. J. Chem.* **1976**, *54*, 617–623.
- (40) Gauss, J.; Stanton, J. J. *Chem. Phys.* **1996**, *104*, 2574–2583.
- (41) Joule, J. A.; Mills, K. *Heterocyclic Chemistry*, 5th ed.; Wiley-Blackwell: Chichester, U.K., 2010; Chapter 25, pp 461–483.
- (42) Beker, W.; Szarek, P.; Komorowski, L.; Lipiński, J. *J. Phys. Chem. A* **2013**, *117*, 1596–1600.